2023-03-16

Passivity-Based Trajectory Tracking and Formation Control of Nonholonomic Wheeled Robots Without Velocity Measurements

Li, N

10.1109/tac.2023.3258320
IEEE Transactions on Automatic Control
Institute of Electrical and Electronics Engineers (IEEE)

Passivity-based Trajectory Tracking and Formation Control of Nonholonomic Wheeled Robots Without Velocity Measurements

Ningbo Li, Pablo Borja, *Member, IEEE,* Jacquelien M.A. Scherpen, *Fellow, IEEE,* Arjan van der Schaft, *Fellow, IEEE,* Robert Mahony, *Fellow, IEEE*

***Abstract*—This note proposes a passivity-based control method for trajectory tracking and formation control of nonholonomic wheeled robots without velocity measurements. Coordinate transformations are used to incorporate the nonholonomic constraints, which are then avoided by controlling the front end of the robot rather than the center of the wheel axle into the differential equations. Starting from the passivity-based coordination design, the control goals are achieved via an internal controller for velocity tracking and heading control and an external controller for formation in the port-Hamiltonian framework. This approach endows the resulting controller with a physical interpretation. To avoid unavailable velocity measurements or unreliable velocity estimations, we derive the distributed control law with only position measurements by introducing a dynamic extension. In addition, we prove that our approach is suitable not only for acyclic graphs but also for a class of non-acyclic graphs, namely, ring graphs. Simulations are provided to illustrate the effectiveness of the approach.**

***Index Terms*—Passivity, wheeled robots, port-Hamiltonian, nonholonomic constraints**

I. Introduction

Recently, there has been an increasing interest in the formation control of multi-robot systems, giving rise to numerous studies on this topic such as the surveys [1], [2], [3] and the references therein. This note considers trajectory tracking and formation control of a network of nonholonomic wheeled robots.

The existing literature on formation control and trajectory tracking can be classified into two groups. First, the references where the formation trajectory tracking, for fully actuated systems, such as single or double integrator models, is achieved for time-varying linear and angular velocities, e.g., [4], [5], [6]. Second, the references that consider wheeled robots with nonholonomic constraints, where the formation trajectory tracking can be achieved for a specific constant heading and an unspecified forward velocity (e.g., [7], [8]) or in a leader-follower strategy (e.g., [9], [10], [11], [12], [13], [14]). Notably, in the approaches that adopt the leader-follower strategy, the prescribed information of the leaders are known to the follower through measuring or communication, and the followers achieve formation control and trajectory tracking of the whole group. In [10], the parallel heading formation and vanishing trajectory was considered, while in [11], the case of communication constraints was investigated. Both papers assume that the robots have access to velocity measurements. However, velocity sensors are expensive and may introduce additional errors. To avoid this issue, several kinds of observers were proposed in [12], [13], [14]. Furthermore, introducing observers may increase the complexity of the analysis and control design due to the nonlinear nature of the system to be controlled. In contrast to the approaches mentioned above, we consider the leaderless formation control and trajectory tracking simultaneously without using velocity measurements or implementing observers.

In this note, we model the network of wheeled robots in port-Hamiltonian (pH) form [15]. In contrast to other modeling approaches where the agents are modeled as single or double integrators, the pH framework is suitable to represent complex and heterogeneous agent dynamics. Furthermore, pH models are convenient in terms of scalability [16], making them suitable to represent complex networks. Since in this modeling framework the dissipation and the energy of the system are underscored, passivity-based control techniques arise as a natural option to control pH systems. In particular, passivity-based decentralized controllers allow the agents to exert forces based on relative information with respect to their neighbors, such as relative position, distance, and bearing. In this control approach, virtual springs determine the formation by shaping the energy function of the network, while the transient response is modified by virtual dampers that inject damping into the network.

Due to the nonholonomic constraints on the wheel axle, there exists no continuous state feedback to stabilize the robot dynamics [17]. In order to solve the stabilization problem, discontinuous control laws [18] and time-varying control laws [19] have been proposed. To deal with the nonholonomic constraints in the pH form, we first use a coordinate transformation [20] to incorporate the algebraic constraints into the differential equations. Controlling the front end of the wheeled robot rather than the center of the wheel axle is a common technique to deal with nonholonomic constraints. Then, we combine this technique with virtual couplings by changing the assigning point to the front end of the robot. We remark

Ningbo Li, Jacquelien M.A. Scherpen, and Arjan van der Schaft are with the Faculty of Science and Engineering, University of Groningen, 9747 AG Groningen, The Netherlands. (e-mail: ningbo.li@rug.nl, j.m.a.scherpen@rug.nl, a.j.van.der.schaft@rug.nl).

Pablo Borja is with the School of Engineering, Computing and Mathematics, University of Plymouth, Plymouth, UK. (e-mail: pablo.borjarosales@plymouth.ac.uk).

Robert Mahony is with the Research School of Information Science and Engineering, Australian National University, ACT 2601, Australia (e-mail:robert.mahony@anu.edu.au).

that this approach is not restrictive in practical terms as end effectors and sensors are usually put at the front of the robot.

The starting point for the trajectory tracking and formation control approach proposed in this note is the passivity-based group coordination design given in [21] and the results reported in [22]. In contrast to the mentioned references, we consider that the wheeled robots do not have access to their velocities or relative velocities in this note. This, in principle, hampers the damping injection, which guarantees the convergence of the trajectories or better transitory response. To overcome this issue, we propose a dynamic extension similar to what is done in [23], [24], [25], [26], [27], and extend it to formation networks. This dynamic extension permits injecting damping without velocity measurements or observers. Hence, to address the trajectory tracking and formation control problems simultaneously, we propose a controller that consists of two parts: an internal feedback that guarantees velocity tracking and heading control for every single robot; and a distributed external controller that achieves group coordination.

The passivity-based group coordination design proposed in [21] and [22] only considers acyclic graphs since graphs containing cycles yield undesired equilibria [16]. In this note, we prove that the proposed control law is applicable to acyclic graphs and cyclic ring graphs. One of the main motivations behind this is the fault tolerance of the network, i.e., if one of the robots fails, the remaining graph is still connected as an acyclic graph, and the whole system still works.

The main contributions of this paper are summarized as follows:

- The trajectory tracking and formation control of nonholonomic wheeled robots with the specified velocity and heading are simultaneously considered in the pH form. Moreover, we propose a general closed-loop Hamiltonian for heading control which can address additional issues, such as large control signals.
- Inspired by the results reported in [23], [24], [25], [26], [27], we propose a dynamic extension approach that permits injecting damping into the closed-loop system without measuring velocities while preserving the pH structure. The latter lets us extend the result to the multi-agent case, contrary to the mentioned references where the authors consider only one agent.
- In contrast to [21] and [22], the proposed passivity-based design for formation control is applicable not only to acyclic graphs but also to a class of non-acyclic graphs, namely, ring graphs. Hence, the proposed approach is robust against robot failures.

The rest of the paper is structured as follows. The preliminaries and the problem formulation are given in Section II. The controller design for the control goals with dynamics extension is presented in Section III. Simulations are provided in Section IV, and concluding remarks appear in Section V.

II. Preliminaries and Problem Formulation

A. Preliminaries

The pH systems theory brings together port-based modeling, geometric mechanics, and system and control theory in physical system modeling and analysis, which provides a clear representation of many physical processes. Considering the energy function, the interconnection relation, and the energy-dissipation of the system, the input-state-output pH model [15], [28] is formulated as

$$\begin{aligned} \dot{x} &= (J(x) - R(x))\frac{\partial H}{\partial x}(x) + g(x)u, \\ y &= g^T(x)\frac{\partial H}{\partial x}(x), \end{aligned}$$

where $x \in \mathbb{R}^n$ is the state, $u \in \mathbb{R}^m$ is the input, $y \in \mathbb{R}^m$ is the output, $J(x) = -J^T(x) \in \mathbb{R}^{n\times n}$ is the skew-symmetric interconnection matrix, and $R(x) = R^T(x) \geq 0 \in \mathbb{R}^{n\times n}$ is the positive semi-definite dissipation matrix. $H(x)$ is the Hamiltonian that equals the total energy stored in the system. It is easy to verify that the time derivative of $H(x)$ satisfies that $\dot{H}(x) \leq y^T u$, which leads to the passivity of the system with respect to (u, y) under the assumption that $H(x)$ is bounded from below. Otherwise, the system is cyclo-passive. This passivity property is often used to prove the stability of the closed-loop system. In contrast to other modeling approaches, the pH systems highlight the interconnection structure related to the exchange of energy. This suitable description of systems is essential for passivity-based control, in which most design techniques are achieving control objectives by energy-shaping and damping injection. For more details of passivity-based control and the pH systems, we refer the readers to [29], [15].

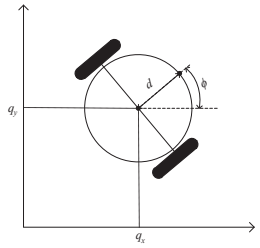

Fig. 1. Wheeled robot with the center of the axle and the front end

B. Problem Formulation

Consider a group of N wheeled robots with an information exchange topology between these robots described by a graph $\mathcal{G}(\mathcal{V}_N, \mathcal{E}_M)$. The incidence matrix $B \in \mathbb{R}^{N\times M}$ describes the relationship between the nodes and the edges, and it takes the following form:

$$b_{ij} = \begin{cases} +1 & \text{if node } i \text{ is at the positive side of edge } j, \\ -1 & \text{if node } i \text{ is at the negative side of edge } j, \\ 0 & \text{otherwise.} \end{cases}$$

In this note, we focus on acyclic graphs, $M = N - 1$ and cyclic ring graphs, $M = N$, where $N \geq 2$. The graphs consist of a node set $\mathcal{V}$, where $\mathcal{V} = \{n_1, n_2, ..., n_N\}$, and an edge set $\mathcal{E} \subseteq \mathcal{V} \times \mathcal{V}$, where $\mathcal{E} = \{e_1, e_2, ..., e_M\}$. The dynamics of each wheeled robot are modeled as a rigid body with a nonholonomic constraint on its axle. Let $q_i = (q_{x_i}, q_{y_i}, \phi_i)^T \in \mathbb{R}^3$, $p_i^{rb} = (p_{x_i}, p_{y_i}, p_{\phi_i})^T \in \mathbb{R}^3$ denote the position and

momentum of the i-th robot respectively. Let $M_i^{rb} = \text{diag}(m_i, m_i, I_{cm_i})$ denote the mass inertia matrix where m_i is the total mass and I_{cm_i} is the moment of inertia around the center of mass of robot i. Let $u_i = (u_{f_i}, u_{\phi_i})^T \in \mathbb{R}^2$ denote the vector of driving input force with forward force u_{f_i} and rotation torque u_{ϕ_i} acting on the axis of rotation. Let $y_i = v_i = (v_{f_i}, v_{\phi_i})^T \in \mathbb{R}^2$ denote the passive output with forward velocity v_{f_i} and angular velocity v_{ϕ_i}. The dynamics of the i-th wheeled robot [15] are given as

$$\begin{aligned}\begin{pmatrix}\dot{q}_i\\ \dot{p}_i^{rb}\end{pmatrix} &= \begin{pmatrix}0 & I_3\\ -I_3 & -D_i^{rb}\end{pmatrix}\begin{pmatrix}\frac{\partial H_i^{rb}}{\partial q_i}(p_i^{rb})\\ \frac{\partial H_i^{rb}}{\partial p_i^{rb}}(p_i^{rb})\end{pmatrix} + \begin{pmatrix}0\\ F(q_i)\end{pmatrix}u_i,\\ y_i &= F^T(q_i)\frac{\partial H_i^{rb}}{\partial p_i^{rb}}(q_i, p_i^{rb}),\end{aligned} \tag{1}$$

with

$$D_i^{rb} = \begin{pmatrix}d_{f_i} & 0 & 0\\ 0 & d_{f_i} & 0\\ 0 & 0 & d_{\phi_i}\end{pmatrix}, F(q_i) = \begin{pmatrix}\cos\phi_i & 0\\ \sin\phi_i & 0\\ 0 & 1\end{pmatrix},$$

where d_{f_i} is the forward viscous friction coefficient, and d_{ϕ_i} is the rotation viscous friction coefficient. The Hamiltonian $H_i^{rb} : \mathbb{R}^3 \mapsto \mathbb{R}$ equals the kinetic energy

$$H_i^{rb}(p_i) = \frac{1}{2}(p_i^{rb})^T(M_i^{rb})^{-1}p_i^{rb}. \tag{2}$$

The nonholonomic constraint on the wheel axle of each robot is given by

$$\dot{q}_{x_i}\sin\phi_i - \dot{q}_{y_i}\cos\phi_i = 0. \tag{3}$$

We restrict our attention to the desired trajectory of the whole group specified by a straight line. Therefore, the control objectives can be reformulated as follows: each wheeled robot tracks a specified velocity $v_i^* = (v_{f_i}^*, 0)^T$ with the nonzero forward velocity $v_{f_i}^*$ and zero angular velocity, i.e., a constant desired heading ϕ_i^*, while the whole group achieves the desired formation shape. Note that to maintain a formation shape, v_i^*, ϕ_i^* should be the same for all the robot $i, i \in \{1, 2, ..., N\}$. Let $z_j := (z_{x_j}, z_{y_j}) \in \mathbb{R}^2$ denote the relative position of the center on x and y axis for two agents connected by an edge j. The desired formation shape is defined by z_j^* for all edges j, $j \in \{1, 2, ..., M\}$. Therefore, the objectives can be summarized as follows

$$\begin{cases}\phi_i(t) \to \phi_i^*\\ v_{f_i}(t) \to v_{f_i}^* \quad as \quad t \to \infty.\\ z_j(t) \to z_j^*\end{cases} \tag{4}$$

III. Main results

In order to eliminate the nonholonomic constraint of the model (1), we use the coordinate transformation [15] $(q_i, p_i^{rb}) \to (q_i, p_i, p_{s_i})$, with $p_i = (p_{f_i}, p_{\phi_i})$, which transforms the rigid body momentum vector p_i^{rb} into the pseudo-momentum vector $(p_{f_i}, p_{\phi_i}, p_{s_i})$, where p_{f_i}, p_{ϕ_i}, and p_{s_i} denote the forward pseudo-momentum, the angular pseudo-momentum, and the constrained sideway pseudo-momentum, respectively. The specific coordinate transformation for the model can be formulated as

$$\begin{pmatrix}p_{f_i}\\ p_{\phi_i}\\ p_{s_i}\end{pmatrix} = \begin{pmatrix}\cos\phi_i & \sin\phi_i & 0\\ 0 & 0 & 1\\ \sin\phi_i & -\cos\phi_i & 0\end{pmatrix}\begin{pmatrix}p_{x_i}\\ p_{y_i}\\ p_{\phi_i}\end{pmatrix} \tag{5}$$

Note that the dynamics of p_{s_i} are eliminated in the new coordinates due to the nonholonomic constraint. Hence, the dynamics of the constrained state space is

$$\begin{aligned}\begin{pmatrix}\dot{q}_i\\ \dot{p}_i\end{pmatrix} &= \begin{pmatrix}0 & S_i(q_i)\\ -S_i^T(q_i) & -D_i^r\end{pmatrix}\begin{pmatrix}\frac{\partial H_i}{\partial q_i}(p_i)\\ \frac{\partial H_i}{\partial p_i}(p_i)\end{pmatrix} + \begin{pmatrix}0\\ I_2\end{pmatrix}u_i\\ H_i(p_i) &= \tfrac{1}{2}p_i^T(M_i^r)^{-1}p_i, \quad y_i = \frac{\partial H_i}{\partial p_i}(p_i),\end{aligned} \tag{6}$$

where $D_i^r := S_i^T(q_i)D_i^{rb}S_i(q_i)$, $M_i^r = \text{diag}(m_i, I_{cm_i})$, and

$$S_i(q_i) = \begin{pmatrix}\cos\phi_i & 0\\ \sin\phi_i & 0\\ 0 & 1\end{pmatrix}.$$

The control objectives are divided into three parts: heading control, forward velocity tracking, and formation control. Correspondingly, the control law is the sum of the three controllers. Moreover, we split the controller into an internal controller for forward velocity tracking and heading control; and an external controller for formation control.

A. Controller design for heading control and forward velocity tracking

The first step in the control design consists in defining the errors of interest $\bar{q}_i = (\bar{q}_{x_i}, \bar{q}_{y_i}, \bar{\phi}_i)^T, \bar{p}_i = (\bar{p}_{f_i}, \bar{p}_{\phi_i})$, which are given by

$$\bar{q}_{x_i} := q_{x_i} - q_{x_i}^*, \quad \bar{q}_{y_i} := q_{y_i} - q_{y_i}^*, \quad \bar{\phi}_i := \phi_i - \phi_i^*,$$

$$\bar{p}_{f_i} := p_{f_i} - p_{f_i}^*, \quad \bar{p}_{\phi_i} := p_{\phi_i} - p_{\phi_i}^*,$$

where $q_{x_i}^*, q_{y_i}^*, \phi_i^*$ are desired positions and $p_{f_i}^*, p_{\phi_i}^*$ are desired momenta. Note that, due to the nonholonomic constraint between the heading and velocity, $\dot{q}_{x_i}^*, \dot{q}_{y_i}^*$ are time-variant during the transition process, and the states $\bar{q}_{x_i}, \bar{q}_{y_i}$ eventually converge to constant values. To obtain the error dynamics, we use the coordinate transformations twice. For heading control, we define the heading error $\hat{\phi}_i = \phi_i - \phi^*$. The positions are transformed from $q_i = (q_{x_i}, q_{y_i}, \phi_i)^T$ to $\hat{q}_i = (q_{x_i}, q_{y_i}, \hat{\phi}_i)^T$, and p_i remains the same. For forward velocity tracking, the following generalized canonical coordinate transformations [30] are introduced to derive the error dynamics:

$$\begin{pmatrix}\bar{q}_i(t)\\ \bar{p}_i(t)\end{pmatrix} = \begin{pmatrix}\hat{q}_i - \left(q_i(0) + \int_0^t \hat{S}_i(\hat{q}_i(\sigma))v_i^*d\sigma\right)\\ p_i - M_i^r v_i^*\end{pmatrix}, \tag{7}$$

where $t \in \mathbb{R}^+$ denotes the time, $\hat{q}_i = (q_{x_i}, q_{y_i}, \hat{\phi}_i)^T$, and

$$\hat{S}_i(\hat{q}_i) = \begin{pmatrix}\cos(\hat{\phi}_i + \phi_i^*) & 0\\ \sin(\hat{\phi}_i + \phi_i^*) & 0\\ 0 & 1\end{pmatrix}.$$

Since $v_i^* = (v_{f_i}^*, 0)^T$, with desired angular velocity $v_{\phi_i}^* = 0$, it follows that $\hat{\phi}_i = \bar{\phi}_i$. In new coordinate $(\bar{q}_i, \bar{p}_i)$, note that $\bar{S}_i(\bar{q}_i) = \hat{S}_i(\bar{q}_i)$.

The open-loop system (6) has no potential energy, which is fundamental to determining the equilibrium point of a mechanical system. Therefore, we need to design a control law that assigns the desired potential $U_i(q_i) : \mathbb{R}^3 \to \mathbb{R}_+$ energy to the error system. While such energy has no fixed structure, for stability purposes, it is convenient to propose it positive definite with respect to zero, i.e.,

$$U_i(0) = 0, \quad U_i(\bar{q}_i) > 0 \ \ \forall \ \bar{q}_i \in \mathbb{R}^3 - \{0\}. \tag{8}$$

To avoid large control signals when the heading error is large, we choose the following desired potential energy

$$U_i(\bar{q}_i) = \frac{1}{2}\bar{q}_{x_i}^2 + \frac{1}{2}\bar{q}_{y_i}^2 + k_i^{\phi} \ln|\cosh \bar{\phi}_i|. \tag{9}$$

where the control gain $k_i^{\phi} > 0$. Moreover, to preserve the physical meaning of the controller, we select the following desired kinetic energy

$$T_i(\bar{p}_i) = \frac{1}{2}\bar{p}_i^T (M_i^r)^{-1} \bar{p}_i. \tag{10}$$

Therefore, the desired Hamiltonian is given by

$$H_i^{hv}(\bar{q}_i, \bar{p}_i) = U_i(\bar{q}_i) + T_i(\bar{p}_i), \tag{11}$$

where the superscript hv stands for heading control plus forward velocity tracking.

The following theorem introduces the control law that addresses the heading stabilization and forward velocity tracking problems.

Proposition 1. Consider the system (6) in closed-loop with

$$u_i^{hv} = -\bar{S}_i^T(\bar{q}_i)\frac{\partial U_i}{\partial \bar{q}_i}(\bar{q}_i) - D_i^r v_i^*, \tag{12}$$

with $U_i(\bar{q}_i)$ given in (9). The closed-loop system tracks the desired forward velocity $v_{f,i}^*$ and desired heading ϕ_i^*.

Proof. Considering the first row of (7) we have

$$\begin{aligned} \dot{\bar{q}}_i &= \bar{S}_i(\bar{q}_i)(M_i^r)^{-1} p_i - \bar{S}_i(\bar{q}_i) v_i^* \\ &= \bar{S}_i(\bar{q}_i)(M_i^r)^{-1} \bar{p}_i, \end{aligned} \tag{13}$$

where we used the definition of the error of velocity. Moreover,

$$\begin{aligned} \dot{\bar{p}}_i &= -D_i^r (M_i^r)^{-1} p_i + u_i^{hv} \\ &= -\bar{S}_i^T(\bar{q}_i)\frac{\partial U_i}{\partial \bar{q}_i}(\bar{q}_i) + D_i^r \left(v_i^* - (M_i^r)^{-1} p_i\right) \\ &= -\bar{S}_i^T(\bar{q}_i)\frac{\partial U_i}{\partial \bar{q}_i}(\bar{q}_i) - D_i^r (M_i^r)^{-1} \bar{p}_i. \end{aligned} \tag{14}$$

Hence, combining (13) and (14), we can express the closed-loop system as a pH system. i.e.

$$\begin{pmatrix} \dot{\bar{q}}_i \\ \dot{\bar{p}}_i \end{pmatrix} = \begin{pmatrix} 0 & \bar{S}_i(\bar{q}_i) \\ -\bar{S}_i^T(\bar{q}_i) & -D_i^r \end{pmatrix} \begin{pmatrix} \dfrac{\partial H_i^{hv}}{\partial \bar{q}_i}(\bar{q}_i, \bar{p}_i) \\ \dfrac{\partial H_i^{hv}}{\partial \bar{p}_i}(\bar{q}_i, \bar{p}_i) \end{pmatrix} \tag{15}$$

where $H_i^{hv}(\bar{q}_i, \bar{p}_i)$ is defined as in (11), with the kinetic and potential energies given by (10) and (9), respectively. Note that $H_i^{hv}(\bar{q}_i, \bar{p}_i)$ satisfies the following

$$\begin{aligned} H_i^{hv}(0) &= 0 \\ H_i^{hv}(\bar{q}_i, \bar{p}_i) &> 0, \ \forall \ (\bar{q}_i, \bar{p}_i) \neq (0, 0). \end{aligned} \tag{16}$$

Take $H_i^{hv}(\bar{q}_i, \bar{p}_i)$ as a candidate Lyapunov function. Its time-derivative is given by

$$\begin{aligned} \dot{H}_i^{hv}(\bar{q}_i, \bar{p}_i) &= \dot{\bar{q}}_i^T \frac{\partial H_i^{hv}}{\partial \bar{q}_i} + \dot{\bar{p}}_i^T \frac{\partial H_i^{hv}}{\partial \bar{p}_i} \\ &= -\bar{p}_i^T (M_i^r)^{-1} D_i^r (M_i^r)^{-1} \bar{p}_i. \end{aligned} \tag{17}$$

Now, by invoking LaSalle's invariance principle, we get that the trajectories of the closed-loop system converge to the largest invariant set such that $\dot{H}_i^{hv} = 0$. On this set $D_i^r (M_i^r)^{-1} \bar{p}_i = 0$, which implies that $\bar{p}_i = 0$ and $\dot{\bar{p}}_i = 0$, i.e., $v_i = v_i^*$. Substituting $\dot{\bar{p}}_i = 0$ and $\bar{p}_i = 0$ into (15) yields

$$\bar{S}_i^T \frac{\partial H_i^{hv}}{\partial \bar{q}_i} = \begin{pmatrix} \bar{q}_{x_i} \cos\phi_i + \bar{q}_{y_i} \sin\phi_i \\ k_i^{\phi} \tanh \bar{\phi}_i \end{pmatrix} = \begin{pmatrix} 0 \\ 0 \end{pmatrix} \tag{18}$$

The second row of (18) implies that $\bar{\phi}_i = 0$ on this invariant set, thus completing the proof. □

Remark 1. Since $p_i = 0$ and $\phi_i = \phi_i^*$ on the invariant set such that $\dot{H}_i^{hv} = 0$, the states $\bar{q}_{x_i}, \bar{q}_{y_i}$ eventually converge to constant values. For the control objective, such values are not relevant. Hence, it is not necessary to prove $\bar{q}_{x_i}, \bar{q}_{y_i}$ converge to zero.

Remark 2. Different choices for $U_i(\bar{q}_i)$ may be used to address additional problems, e.g., transient response of the closed-loop system or saturated control signals. See, for instance, [26]. Note that for the choice proposed in (12), the heading control term vanishes only if the heading error is zero and saturates when the error is large.

Remark 3. To provide a physical interpretation of the controller (12), note that the term

$$-\bar{S}_i^T(\bar{q}_i)\frac{\partial U_i}{\partial \bar{q}_i}(\bar{q}_i)$$

shapes the potential energy of the system. This can be understood as virtual rotational springs that *pull* the robot toward the desired heading. On the other hand, the term $D_i^r v_i^*$ injects virtual damping to preserve the pH structure for the error system.

B. Dynamics extension for formation control

To achieve the desired formation, we design a control law that can be interpreted as virtual springs and virtual dampers that interconnect the agents. In this control approach, the virtual springs ensure the stability of the equilibrium for the closed-loop system, while the virtual dampers are used to guarantee the convergence to this equilibrium and improve the transient performance [15]. Note that the desired Hamiltonian for formation control is equal to the potential energy stored in the spring which is defined as $H_j^f = \frac{1}{2}\bar{z}_j^T K_j^f \bar{z}_j$ with the error

of relative position $\bar{z}_j = z_j - z_j^*$, where $K_j^f = diag(k_{x_j}^f, k_{y_j}^f) \in \mathbb{R}^{2\times 2}$ is the positive spring constants matrix. Based on the idea of virtual couplings, we propose the following control law for each agent.

$$u_i^f = -G_i(\phi_i)(K_j^f \bar{z}_j + D_j^f \dot{\bar{z}}_j), \tag{19}$$

where

$$G_i(\phi_i) = \begin{pmatrix} \cos\phi_i & \sin\phi_i \\ -d\sin\phi_i & d\cos\phi_i \end{pmatrix}$$

is used to change the assigning point from the center of the wheel axle to the front end of the robot. Therefore, the control is not hindered by the constraint on the wheel axle. d denotes the distance between the center of mass and the front end of the robot. In (19), the subscript j denotes the edges connecting the agent i and superscript f denotes the formation control law. The virtual spring term $K_j^f \bar{z}_j$ determines the formation shape, while the virtual damping term $D_j^f \dot{\bar{z}}_j$ with the positive virtual damping constants matrix $D_j^f = diag(d_{x_j}^f, d_{y_j}^f) \in \mathbb{R}^{2\times 2}$ shapes the transient response.

Consider a connected graph $\mathcal{G}(\mathcal{V}_N, \mathcal{E}_M)$ of N wheeled robots. Let B denote the incidence matrix. The whole control input is given by u^{hv} and u^f, where u^{hv} and u^f are the compact form of u_i^{hv} and u_i^f,

$$\begin{aligned} u^w &= u^{hv} + u^f \\ &= -(0_n^T, 1_n^T)^T k^\phi \tan\hat{\phi} - D^r v^* - G(\bar{q})(B\otimes I_2)K^f \bar{z} \\ &\quad - G(\bar{q})(B\otimes I_2)D^f \dot{\bar{z}}, \end{aligned} \tag{20}$$

where $u^w \in \mathbb{R}^{2N}$. Note that in the following part when the subscript i is omitted, it means the state is in compact form for all agents. The dynamics of the closed-loop system in compact form with the controller (20) as input can be described as

$$\begin{pmatrix} \dot{\bar{q}} \\ \dot{\bar{p}} \\ \dot{\bar{z}} \end{pmatrix} = \begin{pmatrix} 0 & \bar{S}(\bar{q}) & 0 \\ -\bar{S}^T(\bar{q}) & -\bar{D}(\bar{q}) & -G^*(\bar{q}) \\ 0 & G^{*T}(\bar{q}) & 0 \end{pmatrix} \begin{pmatrix} \frac{\partial H^w}{\partial \bar{q}}(\bar{q},\bar{p},\bar{z}) \\ \frac{\partial H^w}{\partial \bar{p}}(\bar{q},\bar{p},\bar{z}) \\ \frac{\partial H^w}{\partial \bar{z}}(\bar{q},\bar{p},\bar{z}) \end{pmatrix},$$

where $G^*(\bar{q}) = G(\bar{q})(B\otimes I_2)$, and

$$\bar{D}(\bar{q}) = D^r + G^*(\bar{q})D^f G^{*T}(\bar{q}).$$

The corresponding desired Hamiltonian is

$$H^w(\bar{q},\bar{p},\bar{z}) = H^{hv}(\bar{q},\bar{p}) + H^f(\bar{z}).$$

Note that the superscript w in H^w and u^w denotes that the control law and Hamiltonian are derived considering that the relative velocity is measurable. In particular, the control law (20) depends on the relative velocity. However, velocity sensors are expensive and may introduce additional errors. To avoid these issues, we propose a control law that does not require velocity measurements.

In control practice, to avoid relying on the unavailable velocity measurement or unreliable velocity estimates, the following so-called dirty-derivatives filter [25] in the frequency domain can be introduced as

$$\nu = \frac{b}{s+a}\dot{q} \quad \Leftrightarrow \quad \nu = \frac{bs}{s+a}q, \tag{21}$$

where a, b are parameters of the filter, s is corresponding to the $\frac{d}{dt}$ operator in time domain. q is the position measurement and ν can be used to replace the velocity term. Define x_c as the state of the controller and assume $\nu = x_c + bq$, we have the dynamic position-feedback controller in the time domain as

$$\dot{x}_c = -a(x_c + bq), \tag{22}$$

whose output $u_c = -k_1 q - k_2 \nu$ is usually used as the input for the plant, where k_1 and k_2 are corresponding control gains.

The robots do not have access to their velocity or relative velocity, that is, implementing the control input (20) without relying on the relative velocity $\dot{z}$. The term $\dot{\bar{z}}$ is used to improve the rate at which the system converges to the desired formation. Using the idea of (21) and (22), we design the following dynamics of the relative position feedback controller:

$$\dot{z}^d := K^c(\bar{z} - K^d z^d), \tag{23}$$

where $K^c, K^d \in \mathbb{R}^{2M\times 2M}$ are positive-definite diagonal matrices. Define $K^c(\bar{z} - K^d z^d)$ as the output of the controller dynamics (23) and use this to replace the unavailable relative velocity, the new control input is given by

$$u := -\begin{pmatrix} \bar{q}_x\cos\phi + \bar{q}_y\sin\phi \\ k^\phi \tanh\bar{\phi} \end{pmatrix} - G(\bar{q})(B\otimes I_2)K^v\bar{z} + u^d, \tag{24}$$

where $u \in \mathbb{R}^{2N}$, $u^d = -G(\bar{q})(B\otimes I_2)D^f K^c(\bar{z} - K^d z^d)$. Define the desired Hamiltonian as

$$H(\bar{q},\bar{p},\bar{z},z^d) = H^w(\bar{q},\bar{p},\bar{z}) + \frac{1}{2}(\bar{z} - K^d z^d)^T K^c(\bar{z} - K^d z^d). \tag{25}$$

The closed-loop system with control input (24) can be described as

$$\begin{aligned} \begin{pmatrix} \dot{\bar{q}} \\ \dot{\bar{p}} \\ \dot{\bar{z}} \\ \dot{z}^d \end{pmatrix} &= \begin{pmatrix} 0 & \bar{S}(\bar{q}) & 0 & 0 \\ -\bar{S}^T(\bar{q}) & -\bar{D}^r(\bar{q}) & -G^*(\bar{q}) & 0 \\ 0 & G^{*T}(\bar{q}) & 0 & 0 \\ 0 & 0 & 0 & -(K^d)^{-1} \end{pmatrix} \\ &\quad \times \begin{pmatrix} \frac{\partial H}{\partial \bar{q}}(\bar{q},\bar{p},\bar{z},z^d) \\ \frac{\partial H}{\partial \bar{p}}(\bar{q},\bar{p},\bar{z},z^d) \\ \frac{\partial H}{\partial \bar{z}}(\bar{q},\bar{p},\bar{z},z^d) \\ \frac{\partial H}{\partial \bar{z}^d}(\bar{q},\bar{p},\bar{z},z^d) \end{pmatrix}. \end{aligned} \tag{26}$$

Theorem 1. Assume that a group of agents modeled in (1) is connected as an acyclic graph or a cyclic ring graph defined in II.B. Using the control law (24), the agents achieve the control objectives provided in (4).

Proof. Take the Hamiltonian $H(\bar{q},\bar{p},\bar{z},z^d)$, given in (25), as a candidate Lyapunov function. Note that $H(\bar{q},\bar{p},\bar{z},z^d) \geq 0$. Moreover, its time derivative is given by

$$\begin{aligned} \dot{H} &= \dot{\bar{q}}^\top \frac{\partial H}{\partial \bar{q}} + \dot{\bar{p}}^\top \frac{\partial H}{\partial \bar{p}} + \dot{\bar{z}}^\top \frac{\partial H}{\partial \bar{z}} + (\dot{\bar{z}}^d)^\top \frac{\partial H}{\partial \bar{z}^d} \\ &= -\bar{p}^T (M^r)^{-1} D^r (M^r)^{-1} \bar{p} \\ &\quad -(\bar{z} - K^d z^d)^\top K^c (\bar{z} - K^d z^d). \end{aligned} \tag{27}$$

Hence, it follows from LaSalle's invariance principle that the system (26) converges to the largest invariant set where $\dot{H} = 0$. Note that on this set $\bar{p} = 0$ and $\bar{z} - K^d z^d = 0$, therefore

$\dot{\bar{p}} = 0$. Substituting $\bar{p} = 0$, $\dot{\bar{p}} = 0$ and $\bar{z} - K^d z^d = 0$ into (26), we get the following expression:

$$-\bar{S}^T(\bar{q})\frac{\partial H}{\partial \bar{q}} - G(\bar{q})(B \otimes I_2)\frac{\partial H}{\partial \bar{z}} = 0. \tag{28}$$

Note that $G(\bar{q})$ is invertible, with

$$G^{-1}(\bar{q}) = \frac{1}{d}\begin{pmatrix} d\cos(\bar{\phi}+\phi^*) & -\sin(\bar{\phi}+\phi^*) \\ d\sin(\bar{\phi}+\phi^*) & \cos(\bar{\phi}+\phi^*) \end{pmatrix}, \tag{29}$$

where d is the distance between the center of mass and the front end of the robot. Premultiplying (28) by $dG^{-1}(\bar{q})$ and rearranging the terms, we get

$$0 = \begin{pmatrix} \sin\phi \\ -\cos\phi \end{pmatrix} k^{\phi} \tanh\bar{\phi} - d(B \otimes I_2)K^f \bar{z}. \tag{30}$$

Hence, differentiating (30) we obtain

$$\begin{aligned} \begin{pmatrix} \sin\phi \\ -\cos\phi \end{pmatrix} k^{\phi}\dot{\phi}\tanh\bar{\phi} + \begin{pmatrix} \sin\phi \\ -\cos\phi \end{pmatrix} k^{\phi}\dot{\bar{\phi}}\sec^2\bar{\phi} \\ -d(B \otimes I_2)K^f \dot{\bar{z}} = 0. \end{aligned} \tag{31}$$

Furthermore, according to the closed-loop system (26) and $\bar{p} = 0$ we derive that $\dot{\bar{\phi}} = 0$ and $\dot{\bar{z}} = 0$, hence

$$0 = \begin{pmatrix} \sin\phi \\ -\cos\phi \end{pmatrix} k^{\phi}\dot{\phi}\tanh\bar{\phi}. \tag{32}$$

Note that (32) implies $\dot{\phi}\tanh\bar{\phi} = 0$. Therefore, we conclude that on the largest invariant set such that $\dot{H} = 0$, we have either $\dot{\phi} = 0$ or $\bar{\phi} = 0$.

Suppose that $\dot{\phi} = 0$. Hence the formation is preserved only if $\phi_i^* = \phi_c^*$ for all robots i, where ϕ_c^* is the common desired heading angle. Since we proved that $\dot{\bar{\phi}} = 0$, under the condition $\dot{\phi} = 0$, we have $\dot{\phi}_i^* = \dot{\phi}_c^* = 0$, where $\dot{\phi}_c^*$ is the common desired angular velocity that depends on the desired trajectory. Furthermore, when $\dot{\phi}_c^* = 0$, to preserve a certain formation, it is required that $v_{f_i}^* = v_c^*$, for all robots i, where v_c^* is some common desired forward velocity. Hence, we derive that $\dot{z}_j^* = 0$ for all edges j. Moreover, since we have proved that $\dot{\bar{z}} = 0$, it follows that $\dot{z} = 0$.

Without loss of generality, for the edge j between robot i and robot k we have

$$\begin{aligned} \dot{z}_j &= G^{-1}(\phi_i)\dot{q}_i - G^{-1}(\phi_k)\dot{q}_k \\ &= \begin{pmatrix} \cos\phi_i & -d\sin\phi_i \\ \sin\phi_i & d\cos\phi_i \end{pmatrix}(M^r)^{-1}p_i - \\ &\quad \begin{pmatrix} \cos\phi_k & -d\sin\phi_k \\ \sin\phi_k & d\cos\phi_k \end{pmatrix}(M^r)^{-1}p_k. \end{aligned} \tag{33}$$

Since $\bar{p} = 0$ on the invariant set, it follows that $p_i = p_i^*$ for all robot i. Then we have $(M^r)^{-1}p_i = (M^r)^{-1}p_k = (0,1)^T v_c^*$. Therefore, we have the following equation due to $\dot{z} = 0$

$$\begin{pmatrix} \cos\phi_i - \cos\phi_k & -d(\sin\phi_i - \sin\phi_k) \\ \sin\phi_i - \sin\phi_k & d(\cos\phi_i - \cos\phi_k) \end{pmatrix} v_c^* = 0. \tag{34}$$

Since it is assumed that $v_c^* \neq 0$, (34) implies that $\phi_i = \phi_k$. In addition, the graph of the formation is assumed to be connected, hence ϕ_i and $\bar{\phi}_i$ for all i converge to common values ϕ_c and $\bar{\phi}_c$. Note that the sum of the rows of B is zero, then we sum equations (30) over i to obtain

$$\begin{aligned} 0 &= \sum_{i=1}^{N}\begin{pmatrix} \sin\phi_i \\ -\cos\phi_i \end{pmatrix} k_i^{\phi}\tanh\bar{\phi}_i \\ &= \begin{pmatrix} \sin\phi_c \\ -\cos\phi_c \end{pmatrix}\tanh\bar{\phi}_c \sum_{i=1}^{N} k_i^{\phi}. \end{aligned} \tag{35}$$

Since k_i^{ϕ} is positive, it follows that $\bar{\phi} = 0$. Substituting $\bar{\phi} = 0$ into (30), we have

$$0 = (B \otimes I_2)K^f \bar{z}. \tag{36}$$

Now suppose that $\bar{\phi} = 0$, then following the same reasoning, substituting $\bar{\phi} = 0$ into (30), we get (36).

Since K^f is a positive-definite diagonal matrix, it is concluded from (36) that $\bar{z}$ converges to the set $\{\bar{z}|\bar{z} \in ker(B \otimes I_2)\}$. Now we split the problem into two different kinds of graphs for the formation, namely, acyclic line graphs and cyclic ring graphs.

Case 1: acyclic line graph. If the graph is a connected acyclic line graph, the columns of the incidence matrix B are linearly independent. Therefore the kernel of B is a null set, and it follows that $\bar{z} = 0$.

Case 2: cyclic ring graph. If the graph is a connected cyclic ring graph, the columns of the incidence matrix B are linearly dependent. Thus the kernel of B is not a null set anymore. However, the ring graph is connected and satisfies that $B^T B = BB^T$, which combined with (36) guarantees that

$$\bar{z} \in \mathrm{im}\mathbb{1}_N, \tag{37}$$

where $\mathbb{1}_N$ is the vector of ones of dimension N. Furthermore, $\sum_{j=1}^{N} z_j = 0$ follows from the geometric properties of the ring graph. For the desired ring graph, we also have $\sum_{j=1}^{N} z_j^* = 0$. Therefore, it follows that $\sum_{j=1}^{N} \bar{z}_j = 0$. This in combination with (37) ensures that $\bar{z} = 0$, thus completing the proof. □

IV. Simulations

We verify the effectiveness of Theorem 1 by numerical simulations in Matlab. Consider a network of $N = 3$ wheeled robots whose model parameters are shown in Table I.

TABLE I
Model parameters of wheeled robots

Parameter	Value
Mass $m_i[kg]$	0.167
Inertia $I_{cm,i}[kg \cdot m^2]$	$9.69 \cdot 10^{-5}$
Damping $d_{f,i}[kg/s]$	2
Damping $d_{\theta,i}[kg \cdot m^2/s]$	0.2
Distance $d[m]$	0.06

The three robots are interconnected in an acyclic line graph and a cyclic triangular graph respectively. For the local controllers of heading control and velocity control, the parameters are set as follows: $\phi^* = \frac{\pi}{2}$ rad, $k^{\phi} = 0.1$ kg/s, and $v_{f_i}^* = 0.2$ m/s for $i \in \{1,2,3\}$. For the distributed formation controller where wheeled robots exchange their information, the parameters are set as $k_{x_j}^f = 2$ kg/s^2, $k_{y_j}^f = 2$ kg/s^2, $d_{x_j}^f = 1$ kg/s, $d_{y_j}^f = 1$ kg/s,

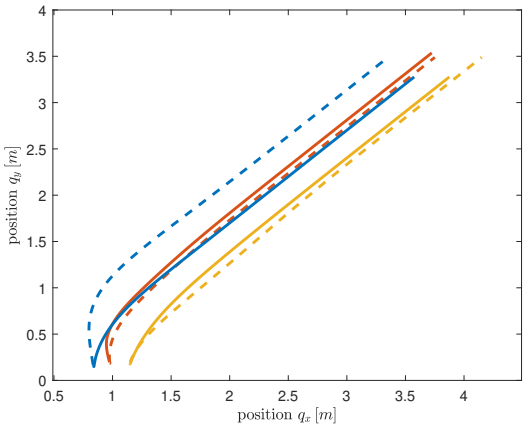

Fig. 2. Trajectories of wheeled robots (dashed lines denote the acyclic line formation and solid lines denote the cyclic triangular formation.)

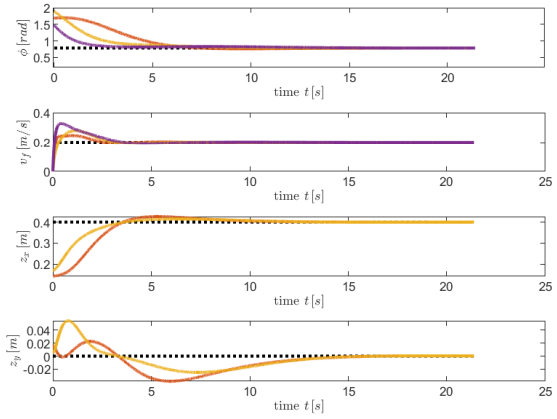

Fig. 3. Time evolution of heading ϕ, forward velocity v_f and relative position of the acyclic line graph

$k^c_{x_j} = 3$ kg/s, $k^c_{y_j} = 3$ kg/s and $k^d_{x_j} = 1$ kg/s, $k^d_{y_j} = 1$ kg/s where $j \in \{1, 2\}$ for acyclic graph and $j \in \{1, 2, 3\}$ for the cyclic graph.

The simulation is performed using MATLAB. The initial conditions of both plots are the same. See Table II.

TABLE II
INITIAL CONDITIONS

Variable	Value
$q_x(0)$	$(0.83, 1.00, 1.15)$ m
$q_y(0)$	$(0.17, 0.19, 0.19)$ m
$\phi(0)$	$(1.68, 1.89, 1.48)$ rad
$p_f(0)$	$(0, 0, 0)$ kg·m/s
$h(0)$	$(0, 0, 0)$ kg·m^2/s

For the desired conditions of two graphs, the line graph is given as $z^*_{x_j} = 0.4$ m, $z^*_{y_j} = 0$ m, $j = 1, 2$ and the triangular graph is given as $z^*_{x_1} = 0.15$ m, $z^*_{x_2} = 0.15$ m, $z^*_{x_3} = -0.3$ m, $z^*_{y_1} = 0.15\sqrt{3}$ m, $z^*_{y_2} = -0.15\sqrt{3}$ m, $z^*_{y_3} = 0$ m.

The trajectories of the wheeled robots are shown in Fig. 2, where the dotted lines are the trajectories of the acyclic line graph and the solid lines are the trajectories of the cyclic triangular graph. The time evolution of heading ϕ, forward velocity v_f and relative positions z_x, z_y of two graphs are shown in Fig. 3 and Fig. 4. The colored lines are the trajectories of the three wheeled robots and the dotted lines are the desired values ϕ^*, v^*_f, z^*_x respectively. While the time evolution of the angular velocity v_ϕ is omitted since it shows a similar trend. Fig. 2 - Fig. 4 show that the heading and the velocity of each wheeled robot converge to the desired value and the desired formation of the group is achieved, which is in accordance with Theorem 1.

In addition to the presented simulations, we have performed simulations with measurement noise included, and the results are very similar.

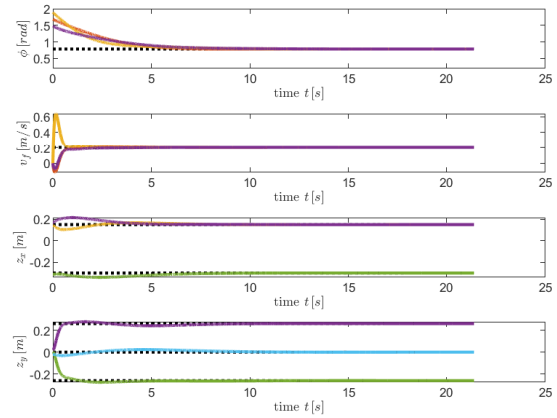

Fig. 4. Time evolution of heading ϕ, forward velocity v_f and relative position of the cyclic triangular graph

V. CONCLUSIONS

In order to achieve trajectory tracking and formation control without velocity measurements, an integrated controller with only relative position feedback is derived. The controller consists of a local heading control part, a forward velocity tracking part, and a distributed formation control part. By introducing a dynamic extension into the controller, the velocity measurements or unreliable velocity estimates are avoided. Simulation results illustrate the effectiveness of the approach.

This paper starts with displacement-based group coordination design, which means each robot can measure relative position based on its own coordinate with the orientation alignment of all the robots. The design is based on the consensus problem in the passivity framework. However, more recently, there is an increasing interest in distance-based and bearing-based formation control, where the rigidity theory plays a key role. Since the pH theory is a powerful tool to study the network dynamics due to the Dirac structure behind it, how to incorporate rigidity formation into the pH framework is an interesting topic for future research [31].

ACKNOWLEDGMENT

The authors would like to thank Geoff Stacey (Australian National University) for the original discussions and notes. The work of Li is supported in part by Xi'an Jiaotong University.

REFERENCES

[1] R. W. Beard, J. Lawton, and F. Y. Hadaegh, "A coordination architecture for spacecraft formation control," *IEEE Transactions on control systems technology*, vol. 9, no. 6, pp. 777–790, 2001.

[2] W. Ren and R. W. Beard, *Distributed consensus in multi-vehicle cooperative control*. Springer, 2008.

[3] K. K. Oh, M. C. Park, and H. S. Ahn, "A survey of multi-agent formation control," *Automatica*, vol. 53, pp. 424–440, 2015.

[4] G. Antonelli, F. Arrichiello, F. Caccavale, and A. Marino, "Decentralized time-varying formation control for multi-robot systems," *The International Journal of Robotics Research*, vol. 33, no. 7, pp. 1029–1043, 2014.

[5] R. Wang, "Adaptive output-feedback time-varying formation tracking control for multi-agent systems with switching directed networks," *Journal of the Franklin Institute*, vol. 357, no. 1, pp. 551–568, 2020.

[6] S. Zhao, Z. Li, and Z. Ding, "Bearing-only formation tracking control of multiagent systems," *IEEE Transactions on Automatic Control*, vol. 64, no. 11, pp. 4541–4554, 2019.

[7] T. Hernandez, A. Loria, E. Nuno, and E. Panteley, "Consensus-based formation control of nonholonomic robots without velocity measurements," in *2020 European Control Conference (ECC)*. IEEE, 2020, pp. 674–679.

[8] E. Nuno, A. Loria, T. Hernandez, M. Maghenem, and E. Panteley, "Distributed consensus-formation of force-controlled nonholonomic robots with time-varying delays," *Automatica*, vol. 120, p. 109114, 2020.

[9] M. A. Maghenem, A. Loria, and E. Panteley, "Cascades-based leader–follower formation tracking and stabilization of multiple nonholonomic vehicles," *IEEE Transactions on Automatic Control*, vol. 65, no. 8, pp. 3639–3646, 2020.

[10] A. Roza, M. Maggiore, and L. Scardovi, "A smooth distributed feedback for formation control of unicycles," *IEEE Transactions on automatic control*, vol. 64, no. 12, pp. 4998–5011, 2019.

[11] S.-L. Dai, S. He, X. Chen, and X. Jin, "Adaptive leader–follower formation control of nonholonomic mobile robots with prescribed transient and steady-state performance," *IEEE Transactions on Industrial Informatics*, vol. 16, no. 6, pp. 3662–3671, 2019.

[12] H. A. Poonawala, A. C. Satici, and M. W. Spong, "Leader-follower formation control of nonholonomic wheeled mobile robots using only position measurements," in *2013 9th Asian Control Conference (ASCC)*. IEEE, 2013, pp. 1–6.

[13] Y. Cheng, R. Jia, H. Du, G. Wen, and W. Zhu, "Robust finite-time consensus formation control for multiple nonholonomic wheeled mobile robots via output feedback," *International Journal of Robust and Nonlinear Control*, vol. 28, no. 6, pp. 2082–2096, 2018.

[14] J. Yang, F. Xiao, and T. Chen, "Event-triggered formation tracking control of nonholonomic mobile robots without velocity measurements," *Automatica*, vol. 112, p. 108671, 2020.

[15] A. J. van der Schaft and D. Jeltsema, "Port-Hamiltonian systems theory: An introductory overview," *Foundations and Trends® in Systems and Control*, vol. 1, no. 2-3, pp. 173–378, 2014.

[16] A. J. van der Schaft and B. M. Maschke, "Port-Hamiltonian systems on graphs," *SIAM Journal on Control and Optimization*, vol. 51, no. 2, pp. 906–937, 2013.

[17] R. W. Brockett *et al.*, "Asymptotic stability and feedback stabilization," *Differential geometric control theory*, vol. 27, no. 1, pp. 181–191, 1983.

[18] D. Lee and K. Y. Lui, "Passive configuration decomposition and passivity-based control of nonholonomic mechanical systems," *IEEE Transactions on Robotics*, vol. 33, no. 2, pp. 281–297, 2016.

[19] C. Samson, "Time-varying feedback stabilization of car-like wheeled mobile robots," *The International journal of robotics research*, vol. 12, no. 1, pp. 55–64, 1993.

[20] A. J. van der Schaft and B. M. Maschke, "On the Hamiltonian formulation of nonholonomic mechanical systems," *Reports on mathematical physics*, vol. 34, no. 2, pp. 225–233, 1994.

[21] M. Arcak, "Passivity as a design tool for group coordination," *IEEE Transactions on Automatic Control*, vol. 52, no. 8, pp. 1380–1390, 2007.

[22] E. Vos, A. J. van der Schaft, and J. M. A. Scherpen, "Formation control and velocity tracking for a group of nonholonomic wheeled robots," *IEEE Transactions on Automatic Control*, vol. 61, no. 9, pp. 2702–2707, 2015.

[23] E. Panteley, A. Loria, and A. Teel, "Relaxed persistency of excitation for uniform asymptotic stability," *IEEE Transactions on Automatic Control*, vol. 46, no. 12, pp. 1874–1886, 2001.

[24] D. A. Dirksz and J. M. A. Scherpen, "On tracking control of rigid-joint robots with only position measurements," *IEEE Transactions on Control Systems Technology*, vol. 21, no. 4, pp. 1510–1513, 2012.

[25] A. Loria, "Observers are unnecessary for output-feedback control of Lagrangian systems," *IEEE Transactions on Automatic Control*, vol. 61, no. 4, pp. 905–920, 2015.

[26] T. Wesselink, P. Borja, and J. M. A. Scherpen, "Saturated control without velocity measurements for planar robots with flexible joints," in *2019 IEEE 58th Conference on Decision and Control (CDC)*. IEEE, 2019, pp. 7093–7098.

[27] E. Nuño and R. Ortega, "Achieving consensus of euler–lagrange agents with interconnecting delays and without velocity measurements via passivity-based control," *IEEE Transactions on Control Systems Technology*, vol. 26, no. 1, pp. 222–232, 2017.

[28] V. Duindam, A. Macchelli, S. Stramigioli, and H. Bruyninckx, *Modeling and control of complex physical systems: the port-Hamiltonian approach*. Springer Science & Business Media, 2009.

[29] P. Kokotovic and H. J. Sussmann, "A positive real condition for global stabilization of nonlinear systems," *Systems & Control Letters*, vol. 13, no. 2, pp. 125–133, 1989.

[30] K. Fujimoto, K. Sakurama, and T. Sugie, "Trajectory tracking control of port-controlled Hamiltonian systems via generalized canonical transformations," *Automatica*, vol. 39, no. 12, pp. 2059–2069, 2003.

[31] G. Stacey and R. Mahony, "The role of symmetry in rigidity analysis: A tool for network localization and formation control," *IEEE Transactions on Automatic Control*, vol. 63, no. 5, pp. 1313–1328, 2017.